

See discussions, stats, and author profiles for this publication at: <https://www.researchgate.net/publication/330987062>

Improving Performance Characteristics of Induction Motor through the DTC with Magnetizing Inductance Compensation

Article · December 2018

CITATIONS

0

READS

31

1 author:



Hamdy Mohamed

Marg High Institute For Engineering And Modern Technology

27 PUBLICATIONS 45 CITATIONS

SEE PROFILE

Some of the authors of this publication are also working on these related projects:



high dynamic performance of permanent magnet synchronous motor with field oriented control [View project](#)



Identification of Stator Winding Faults and Remedial Operation of Permanent Magnet Synchronous Motors with Suppress Noise and Ripple [View project](#)

Improving Performance Characteristics of Induction Motor through the DTC with Magnetizing Inductance Compensation

Hamdy Mohamed Soliman

Department of Electrical Power and Machine Engineering
EL Marg High Institute for Engineering and Modern Technology
EL_Marg, Egypt
eldoctorhamdy70@gmail.com

Abstract— This paper aims to improve the performance characteristics of the induction motor through the direct torque control. In this paper, the magnetizing inductance is compensated. To get good performance for the induction motor, two algorithms are constructed. One of them is used to compute the reference torque and the reference of the stator flux through lookup table of the rotor flux. The other algorithm is used to compute the estimated torque and stator flux. The parameters of these algorithms are compared and the errors are introduced to two proportional integrator controllers to verify the best performance. Also, the stator flux angle of the reference algorithm is used to improve the same angle estimating from the other algorithm. Improving angle has more reliable for performance characteristics of induction motor at low speed and at resistances variation and at any operating conditions.

Keywords— induction motor, algorithms, performance characteristics, direct torque control.

I. INTRODUCTION

The direct torque control (DTC) is spread in the industrial applications due to have some advantages as very simple control, decoupled control of torque and flux, quick torque response, very good dynamic performance, less effective by parameters change, low computational time and absence coordinate transformation. Also, it has some disadvantages as possible problem during starting, torque and flux estimators are needed, higher ripples in torque and flux also current distortions are higher [1-2]. The problems of DTC are arising due to use hysteresis band to control the switching frequency of inverter to drive the AC motor. The basic principle of the DTC is comparing between the reference stator flux and estimated stator flux and the error between them is introduced into hysteresis band also the reference torque is compared to estimated torque and the error is introduced to another hysteresis band [3-4]. This basic principle is constructed to control the AC motor and it is called now the conventional DTC. Fig.1 shows this conventional construction of DTC. If effects of these bands are studied in the conventional DTC it is found that, each band has own effect. The hysteresis band of the stator flux has more influence on the THD of the current which means effecting copper losses of AC machine so when the amplitude of this band increases the THD and copper losses increase. Also, the other hysteresis band is more effecting on the switching frequency of inverter so when amplitude of the band decreases the losses comes from inverter increase [5-6]. To decrease these disadvantages, this paper studied this problem and produced proposal to solve it.

This proposal can be seen in Fig.2. The AC machine used here is the induction motor. In this proposal, the reference value of the stator flux as the magnitude and angle are computed through the rotor flux and reference torque. The rotor flux is deduced from lookup table and reference torque is deduced through proportional integrator (PI) speed controller. The error between the magnitude of the reference stator flux and the magnitude of the estimated stator flux is introduced into the PI flux controller to improve the performance of the flux controller hysteresis band. Also, the error between the reference torque and the estimated torque is introduced into the PI torque controller to improve the performance of the torque controller hysteresis band. To make this proposal more reliable, the reference stator flux angle is used to improve the estimating stator flux angle. Moreover, the magnetizing inductance is compensated. This occurs through the calculation of the airgap flux producing current. This driving model is simulated through the MATLAB program. The simulation shows effectiveness of this driving model and importance of each adding in this model.

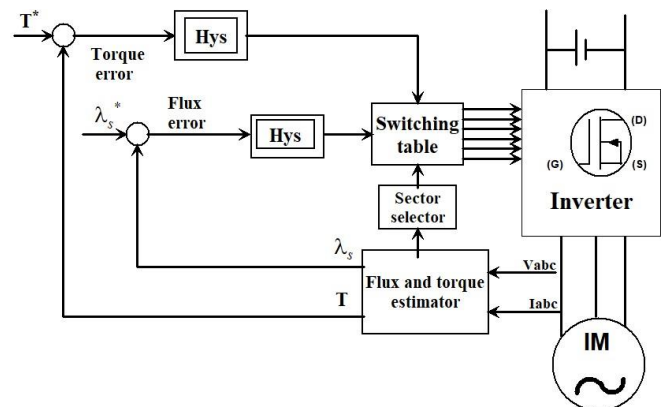


Fig. 1 Conventional method of DTC to drive AC motor

II. INDUCTION MOTOR MODEL

The dynamic model of induction motor in the stationary reference frame can be written as it is

$$v_s = R_s i_s + p \lambda_s \quad (1)$$

$$v_r = R_r i_r + p \lambda_r - j \omega_r \lambda_r \quad (2)$$

$$\lambda_s = L_s i_s + L_m i_r \quad (3)$$

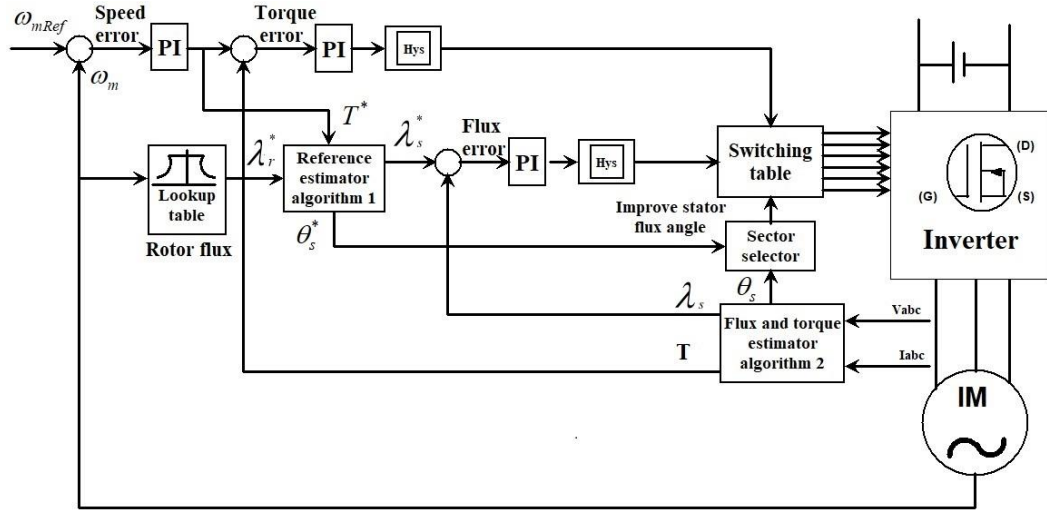


Fig. 2 Proposal induction motor drive system through DTC

$$\lambda_r = L_m i_s + L_r i_r \quad (4)$$

$$Jp\omega_m = T_e - T_L - B\omega_m \quad (5)$$

Where $v_s = [v_{ds} \ v_{qs}]^T$ and $v_r = [v_{dr} \ v_{qr}]^T$ are a space vector of the stator voltage and a rotor voltage respectively, $i_s = [i_{ds} \ i_{qs}]^T$ and $i_r = [i_{dr} \ i_{qr}]^T$ are a space vector of the stator current and a rotor current respectively, $\lambda_s = [\lambda_{ds} \ \lambda_{qs}]^T$ and $\lambda_r = [\lambda_{dr} \ \lambda_{qr}]^T$ are a space vector of the stator flux and a rotor flux respectively, R_s is the stator resistance, R_r is the rotor resistance, L_s is the stator inductance, L_m is the magnetizing inductance, L_r is the rotor inductance, T_e is the electromagnetic motor torque, T_L is the load torque, ω_m is mechanical speed of the motor, B is the fractional coefficient, J is the moment of inertia and p is the deferential operator.

Also, the electromagnetic motor torque can be expressed as

$$T_e = \frac{3}{4}P(\lambda_{ds}i_{qs} - \lambda_{qs}i_{ds}) \quad (6)$$

Where P is the number of poles

III. ALGORITHMS TO IMPROVE THE PERFORMANCE

To improve the performance characteristics of the induction motor through the drive system, two algorithms are used as shown in Fig.2. The first algorithm is used to compute the stator flux as the magnitude and angle depending upon rotor flux from lookup table and reference torque. By written the modeling of induction motor in the synchronous reference frame and locking the rotor flux aligned with d-axis, the electromagnetic torque and q-axis stator and rotor currents can be written as

$$T_e^* = \frac{3}{4}P \frac{L_m}{L_r} \lambda_r^* i_{qs}^* \quad (7)$$

$$i_{qs}^* = -\frac{\omega_r^* L_r}{R_r L_m} \lambda_r^* \quad (8)$$

$$i_{qr}^* = \frac{\omega_r^*}{R_r} \lambda_r^* \quad (9)$$

From “(7-8)” the electrical rotor speed can be written as

$$\omega_r^* = -\frac{4R_r T_e^*}{3P(\lambda_r^*)^2} \quad (10)$$

From “(8-10)” the q-axis stator flux can be written as

$$\lambda_{qs}^* = \frac{4\sigma_x T_e^*}{3P\lambda_r^*} \quad (11)$$

$$\text{Where } \varsigma_x = \frac{L_s L_r}{L_m} - L_m$$

By similar manner, the d-axis stator flux can be written as

$$\lambda_{ds}^* = \frac{L_s}{L_m} \lambda_r^* + \frac{\sigma_x}{R_r} \frac{d}{dt} \lambda_r^* \quad (12)$$

$$\lambda_s^* = \sqrt{\lambda_{ds}^{*2} + \lambda_{qs}^{*2}} \quad (13)$$

$$\theta_s^* = \tan^{-1} \left[\frac{\lambda_{qs}^*}{\lambda_{ds}^*} \right] \quad (14)$$

Where λ_s^* is a magnitude of reference stator flux computed and θ_s^* is computed angle of reference stator flux

The second algorithm is used to estimate the stator flux as the magnitude, angle and electromagnetic torque depending upon the motor current and motor voltage as it is

$$\lambda_{ds} = \int (v_{ds} - i_{ds} R_s) dt \quad (15)$$

$$\lambda_{qs} = \int (v_{qs} - i_{qs} R_s) dt \quad (16)$$

$$\lambda_s = \sqrt{(\lambda_{ds})^2 + (\lambda_{qs})^2} \quad (17)$$

$$\theta_s = \tan^{-1} \left(\frac{\lambda_{qs}}{\lambda_{ds}} \right) \quad (18)$$

The estimated electromagnetic can be found as “(6)”

θ_s is estimating angle of the estimating stator flux (Algorithm 2)

The computing stator flux from algorithm 1 is compared to estimating stator flux from algorithm 2 and the error is introduced to PI flux controller to improve the input of hysteresis band of stator flux, the reference torque from output of the PI speed controller is compared to estimated torque from algorithm 2 and the error is introduced to PI torque controller to improve the input of hysteresis band of torque also the stator flux angle is computed from algorithm 1 is used to improve the stator flux angle estimating from algorithm 2 to improve performance of sector selector which is used with help of hysteresis bands for torque and stator flux to improve the switching of the drive system. This improvement in the stator flux angle will reflect on the dynamic performance and steady state performance of the induction motor at any speed as can be concluded that from simulation results.

IV. MAGNETIZING INDUCTANCE CALCULATION

Here, the magnetizing inductance is reported as the function of magnetizing current. This function is constructed inside the MATLAB program depends upon curve fitting. This function is computed with help of magnetizing voltage, current and reactive power as shown in Fig. 3

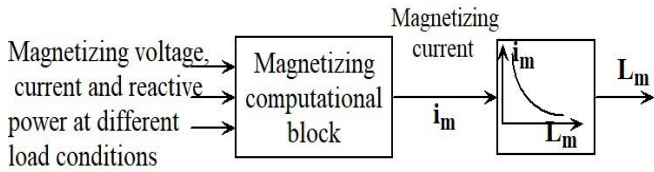


Fig. 3 open loop magnetizing inductance calculation

V. SECTOR SELECTOR

Choosing the appropriate sector is very important in the operation of the DTC. This depends upon the estimated value of the stator flux angle. This is because the performance of the AC motor is related by the shape of the flux. This flux depends upon the space vector of inverter. Due to the stator flux ideally follows circular pass in the space so the stator flux locus can be divided this pass into six sectors (Fig.4) depending upon the active space voltage vector which deduced from the inverter. To determine the position of voltage vectors for inverter, the sector selector block defines the sector specified for the voltage vector belong to it. With increasing or decreasing the stator flux depending upon the hysteresis flux band, the sector selector determines the different set of the vectors for these increasing or decreasing in the stator flux. The hysteresis bands for the stator flux and the torque are quite difference where the flux controller is two level comparators while the torque controller is three level comparators this can be seen in Fig. 5. These comparators can be explained as the follows

For the stator flux, if the reference value greater than the actual value, the output is 1 but if the reference value smaller than the actual value, the output is -1 and this can express as

$$H_\lambda = 1 \quad \text{if} \quad \lambda_s^* > \lambda_s \quad (19)$$

$$H_\lambda = -1 \quad \text{if} \quad \lambda_s^* < \lambda_s \quad (20)$$

For the torque, if the reference value greater than the actual value, the output is 1, if the reference value smaller than the

actual value, the output is -1 and if the reference value and actual value are equal doesn't anything. This can express as

$$H_T = 1 \quad \text{if} \quad T^* > T \quad (21)$$

$$H_T = -1 \quad \text{if} \quad T^* < T \quad (22)$$

$$H_T = 0 \quad \text{if} \quad T^* = T \quad (23)$$

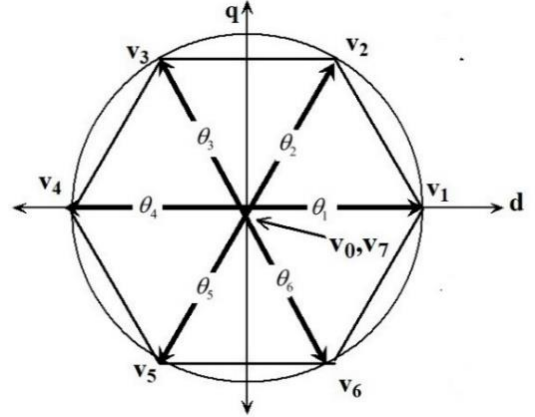


Fig. 4 Sectors and angles

These hysteresis bands and sector selector form the action of the switching table.

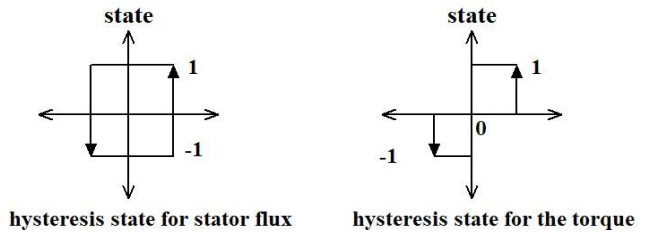


Fig. 5 Hysteresis band for the stator flux and torque

VI. SWITCHING TABLE TO DRIVE THE INVERTER

The hysteresis comparators of the torque and stator flux with help of selector sector are used by switching table block to choose the suitable voltage. The switching table can be seen in table I. Each power switch of inverter operates for duration 180° conducting mode. If the upper switch in the upper leg in any phase is on, the switching signal of this phase is designed as S=1 but if the lower switch in the lower leg in any phase is on, the switching signal of this phase is designed as S=0. By this is the way, there are eight of operation for inverter. Two of them are zero space vectors (V_0, V_7) which located at the center of the space vector plane (Fig. 4) and the others ($V_1 - V_6$) are effective vectors and each one from them faraway from the other in space by 60° . Depending upon these criteria, the output of the inverter voltage as the vector can be calculated as

$$v_{inv} = \frac{2v_{dc}}{3} (S_a + S_b + S_c) \quad (24)$$

Where S_a, S_b, S_c are represent switches signals

In this control, the output of the inverter voltage changes only if output of the hysteresis controllers changes their the outputs at the sampling period

TABLE I. SWITCHING TABLE OF INVERTER VECTOR VOLTAGE

H_λ	H_T	First Sector	Second Sector	Third Sector	Fourth Sector	Fifth Sector	Sixth Sector
1	1	V_2	V_3	V_4	V_5	V_6	V_1
	0	V_0	V_7	V_0	V_7	V_7	V_0
	-1	V_6	V_1	V_2	V_3	V_4	V_5
-1	1	V_3	V_4	V_5	V_6	V_1	V_2
	0	V_7	V_0	V_7	V_0	V_7	V_0
	-1	V_5	V_6	V_1	V_2	V_3	V_4

VII. SIMULATION RESULTS AND DISCUSSION

Here the simulation and simulation results are discussed. The simulation starts by simulating the DTC which is model one at low speed without any modification i.e. the PI speed controller to compare between the reference speed and actual speed to deduce the reference torque and two hysteresis bands one is for the stator flux and the other is for the torque. The simulation results for model one is compared to the simulation results of model two. The model two is the same model one and add to it two PI controllers one of them is an introducing of the hysteresis flux controller to improve this hysteresis band and the other PI controller is an introducing of the hysteresis torque controller to improve this hysteresis band. These two models are compared to the third model (proposal model). This third model is as the second model and add to that the improving in the stator flux angle. Improving this angle occurs by subtracting the reference flux angle from the estimating flux angle to improve the performance overall. The purpose of this comparing is to show effectiveness of each adding in the proposal model. Also, the simulation showed the effect of rising temperature on the performance characteristics of induction motor at low speed. This occurs by increasing the rotor and stator resistances to 150% from rated values and study the effect of this rising on the performance characteristics of induction motor. The increasing in the stator and rotor resistances is choosing to simulate the practical case where in any environmental due the motor operates for along time, the motor temperature increases which mean that, the stator and rotor resistances increases. These resistances reach twice the rated value due to raising in motor temperature. These simulations are repeated at rated load rated speed with tacking into account effect of raising temperature.

A. Simulation Results with Low Speed

Here the mechanical load is at the rated but the motor speed is 100 R.P.M. i.e. 10.46 rad/sec. Fig. 6 shows the stator flux with the first model, Fig. 7 shows the stator flux with the second model and Fig. 8 shows the stator flux with the third model. From these Figs can be concluded that

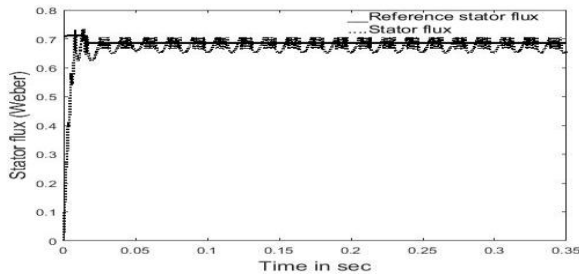


Fig. 6 Stator flux of induction motor with first model

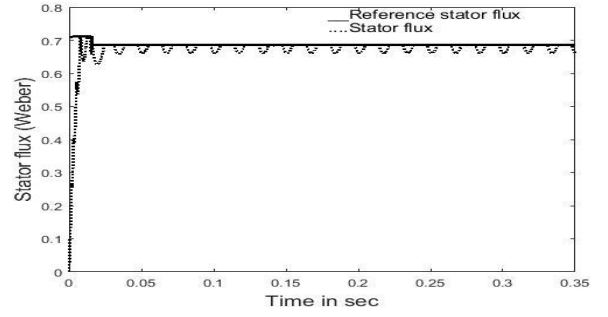


Fig. 7 Stator flux of induction motor with second model

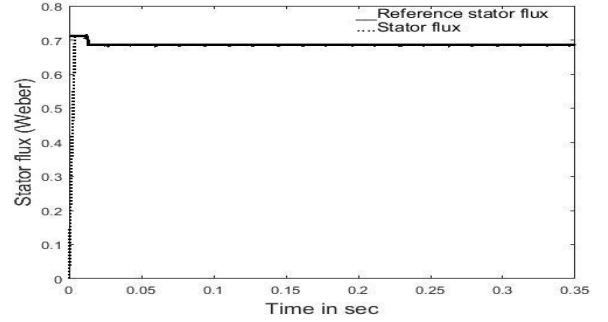


Fig. 8 Stator flux of induction motor with third model

The stator flux is distorted and oscillated with the first model and with the second model if it is compared to the third model. The stator flux is the worst with first model during the dynamic behavior and steady state behavior. The stator flux with third model is the best due to add improvement for computation of the stator flux angle.

Fig. 9 shows the stator current with the first model, Fig. 10 shows the stator current with the second model and Fig. 11 shows the stator current with the third model. From these Figs can be concluded that

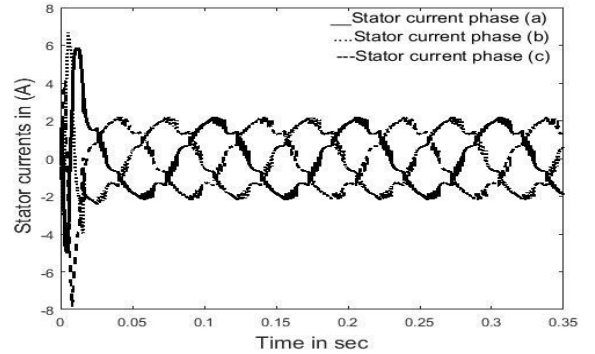


Fig. 9 Stator current of induction motor with first model

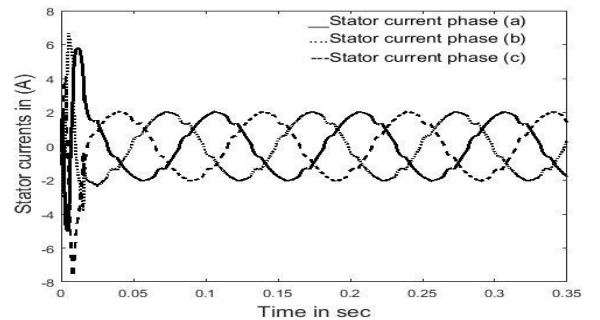


Fig. 10 Stator current of induction motor with second model

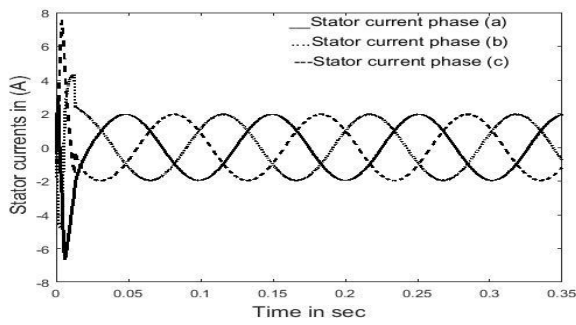


Fig. 11 Stator current of induction motor with third model

The stator current is highly distorted with the first model. This distorted is reduced with the second model and vanish with the third model. This occurs due to improve in the stator flux with third model. This means that, copper losses decrease with third model if it is compared to the first and second models.

The Figs. 12-14 show the effect of these models on the motor torque where it is found that, the dynamic performance is the best with third model if it is compared to the others.

The Figs. 15-17 show the effect of these models on the motor speed where it is found that, the dynamic performance is the best with third model because the motor is less effected by load at starting and reaches to steady speed faster if it is compared to the others models.

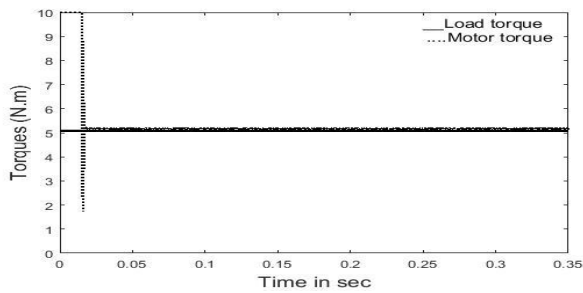


Fig. 12 Torque of induction motor with first model

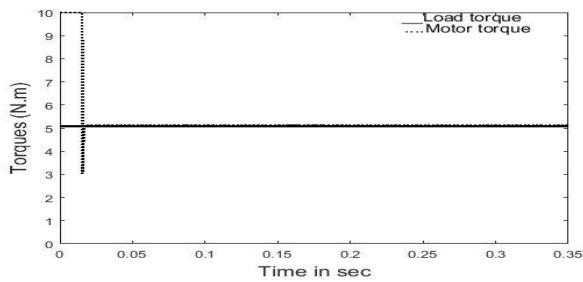


Fig. 13 Torque of induction motor with second model

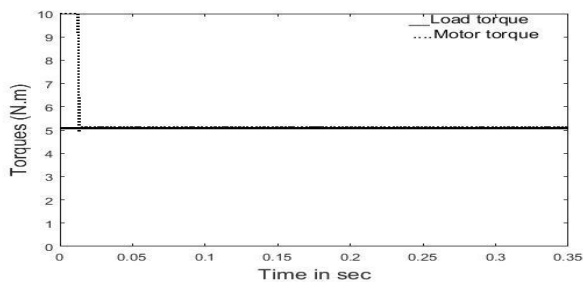


Fig. 14 Torque of induction motor with third model

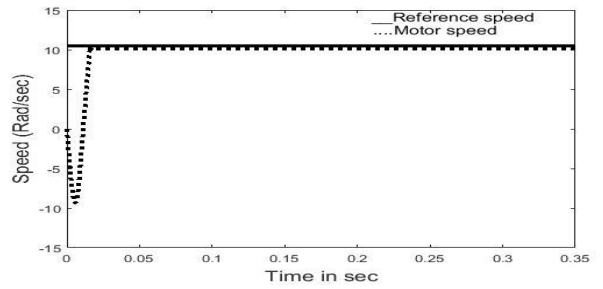


Fig. 15 Speed of induction motor with first model

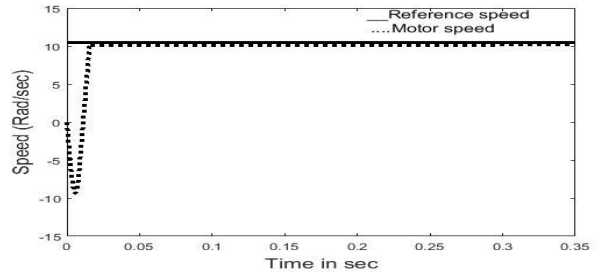


Fig. 16 Speed of induction motor with second model

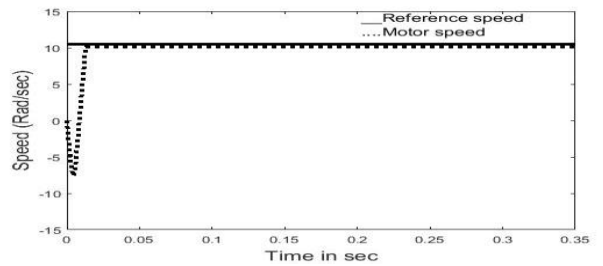


Fig. 17 Speed of induction motor with third model

B. Simulation Results with Low Speed at Rising Temperature

This case as above but the rising temperature is tacking into consideration i.e. rotor and stator resistances increased to 150% of the rated value. Figs. 18-20 show the stator flux for all models. From these Figs can be concluded that

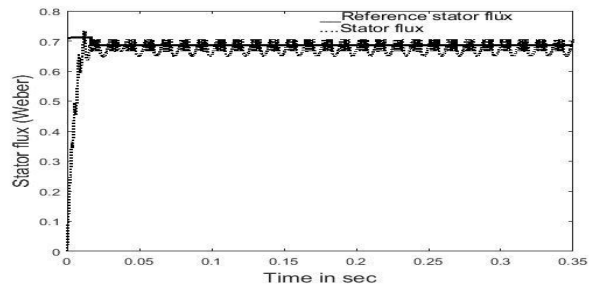


Fig. 18 Stator flux of induction motor with first model

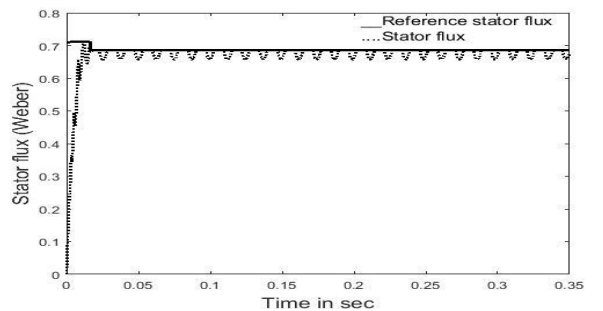


Fig. 19 Stator flux of induction motor with second model

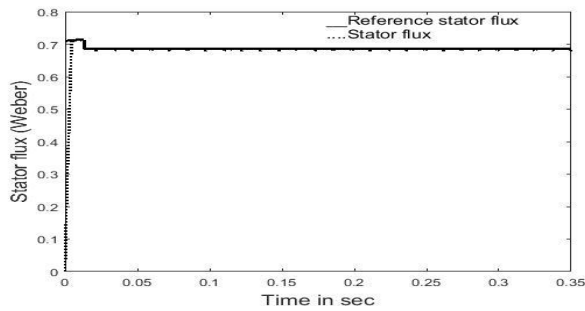


Fig. 20 Stator flux of induction motor with third model

The stator flux is distorted and oscillated with the first model and with the second model if it is compared to the third model. In this case and in the same case without temperature increase, the stator flux is the worst with first model during the dynamic behavior and steady state behavior. The stator flux with third model is the best due to add improvement for computation of the stator flux angle.

Figs. 21-23 shows the stator current with the first model, second model and third model. Where it is found that;

The stator current is highly distorted with the first model if it is compared to others models. This distorted is approximately reduced with the second model and vanish with the third model.

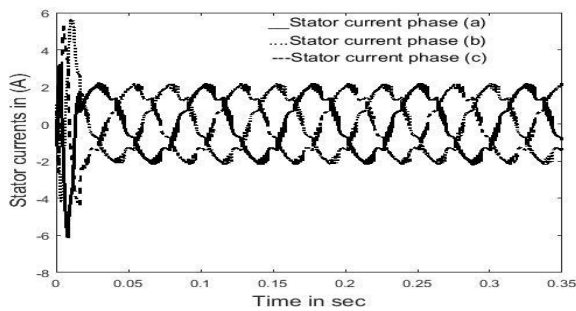


Fig. 21 Stator current of induction motor with first model

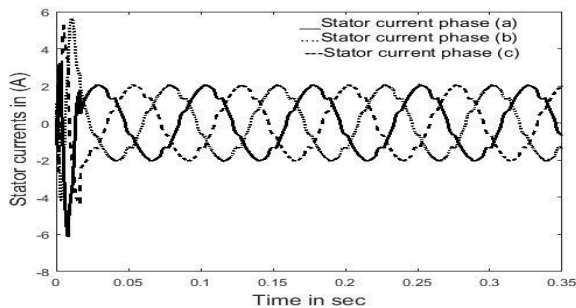


Fig. 22 Stator current of induction motor with second model

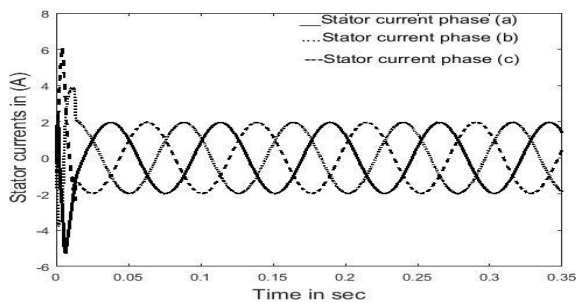


Fig. 23 Stator current of induction motor with third model

The Figs. 24-26 show the effect of these models on the motor torque where it is found that, the dynamic performance is approximately similar for all models.

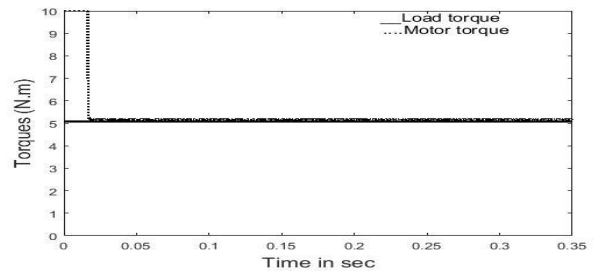


Fig. 24 Torque of induction motor with first model

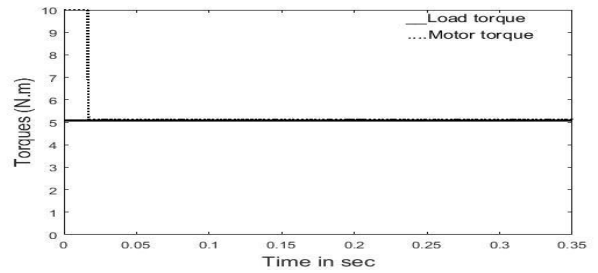


Fig. 25 Torque of induction motor with second model

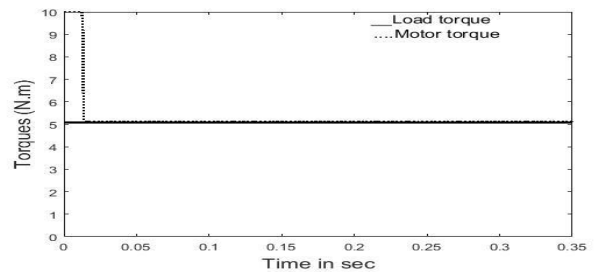


Fig. 26 Torque of induction motor with third model

The Figs. 27-29 show the effect of these models on the motor speed where it is found that, the dynamic performance is the best with third model because the motor is less effected by load at starting if it is compared to the others models.

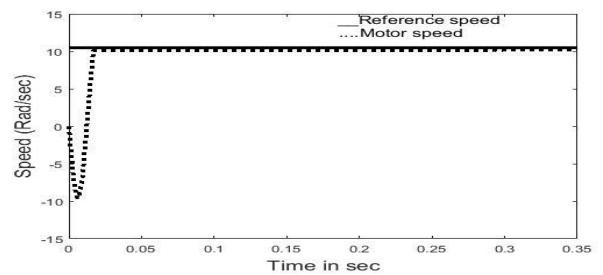


Fig. 27 Speed of induction motor with first model

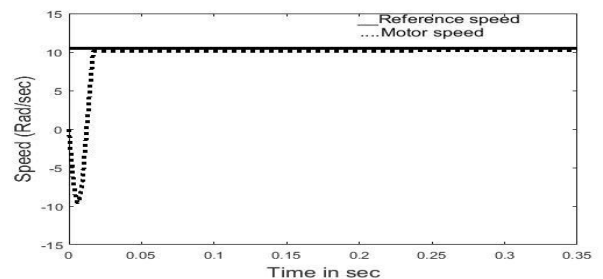


Fig. 28 Speed of induction motor with second model

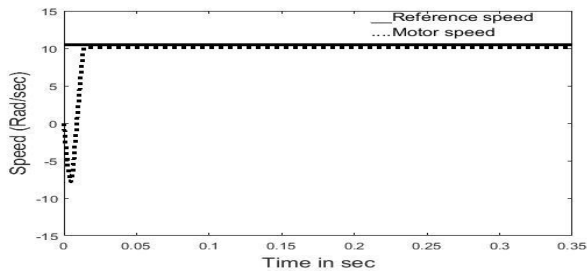


Fig. 29 Speed of induction motor with third model

C. Simulation Results at Rated with Rising Temperature

Here the motor operates at rated condition but the rising temperature is taking into consideration i.e. rotor and stator resistances increased to 150% of the rated value. Figs. 30-32 show the stator flux for all models. From these Figs can be concluded that

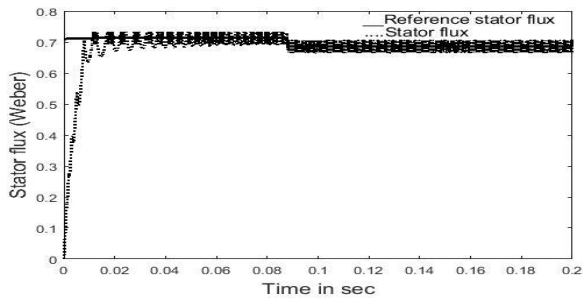


Fig. 30 Stator flux of induction motor with first model

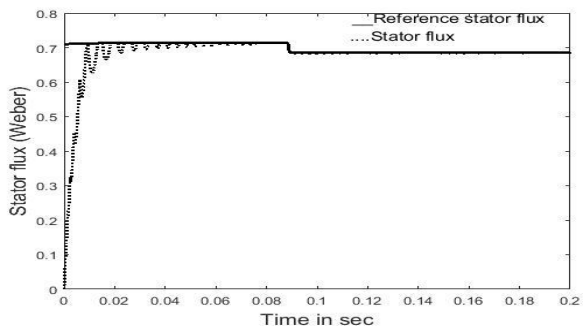


Fig. 31 Stator flux of induction motor with second model

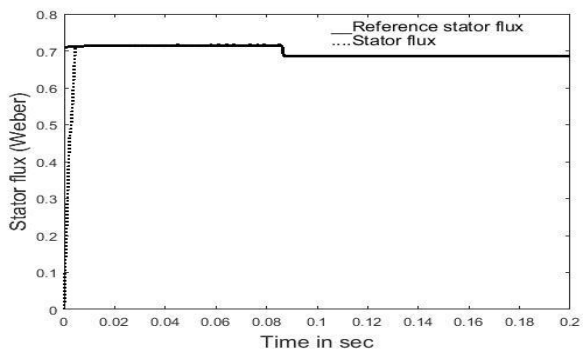


Fig. 32 Stator flux of induction motor with third model

The stator flux is highly distorted with the first model. The stator flux is the worst with first model during the dynamic behavior and steady state behavior. The stator flux with third model is the best.

Figs. 33-35 show the stator current with the first model, second model and third model. Where it is found that;

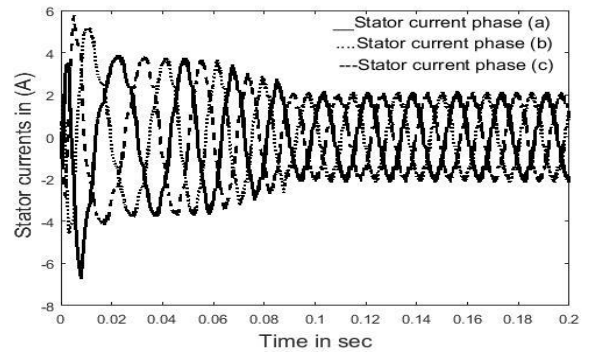


Fig. 33 Stator current of induction motor with first model

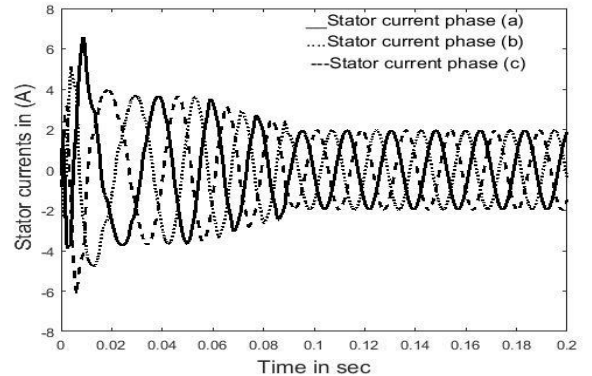


Fig. 34 Stator current of induction motor with second model

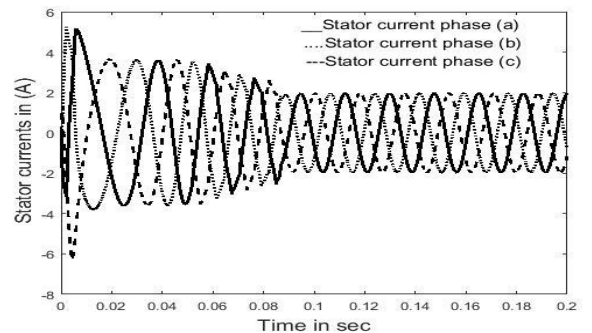


Fig. 35 Stator current of induction motor with third model

The stator current is highly distorted with the first model if it is compared to others models. This distorted is less with the second model and vanish with the third model.

The Figs. 36-38 show the effect of these models on the motor torque where it is found that;

The first model is highly distorted and noisy if it is compared to the others.

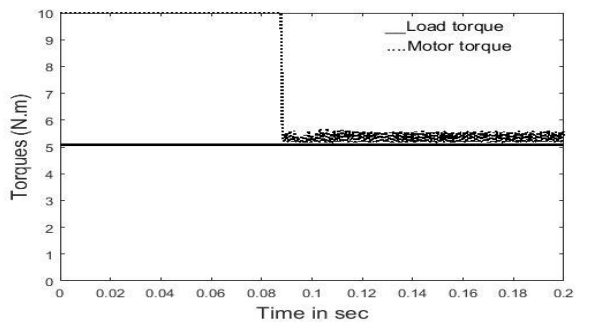


Fig. 36 Torque of induction motor with first model

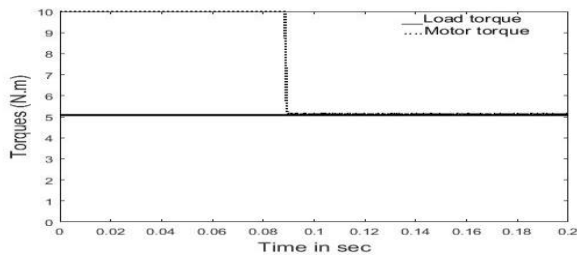


Fig. 37 Torque of induction motor with second model

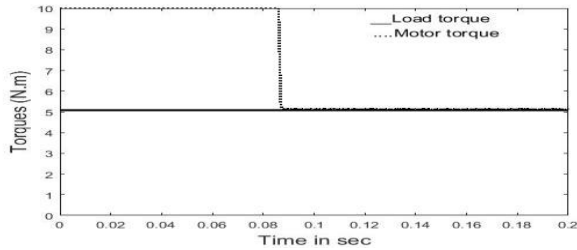


Fig. 38 Torque of induction motor with third model

The Figs. 39-41 show the effect of these models on the motor speed where it is found that, the first model makes more time to reach the steady state speed if it is compared to the others.

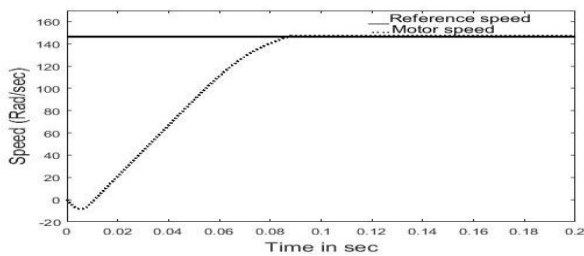


Fig. 39 Speed of induction motor with first model

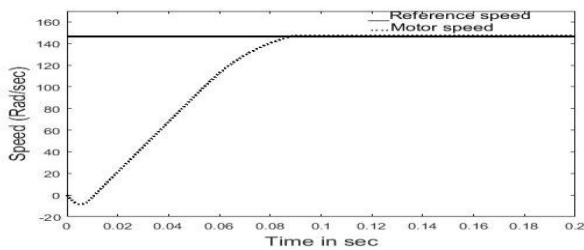


Fig. 40 Speed of induction motor with second model

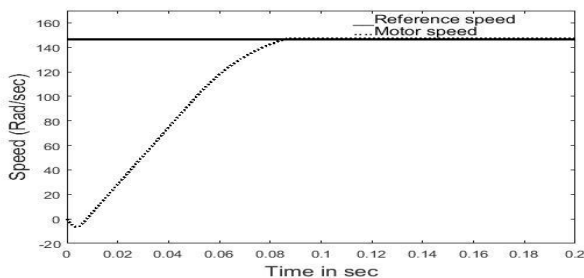


Fig. 41 Speed of induction motor with second model

VIII. CONCLUSIONS

This paper suggested proposal model to improve the performance characteristics of induction motor through the DTC. Some elements are added to the classical DTC such as rotor flux lookup table, PI controllers and modified stator flux

angle. These elements make the model more reliable. Also, the compensating of the magnetizing inductance is constructed. This model improves the stator flux and switching frequency which reflect on the stator current, motor torque and motor speed. These improvements occur at low speed and at rated conditions. This improvement occurs at transient, dynamic and steady state. When this model is tested under high temperature at low and at rated speed gives robust improvement.

TABLE II. MOTOR DATA

Motor Parameters	Values
Power	750 W
Voltage	380 V
Frequency	50 Hz
Poles	4
Speed	1410 RPM
Stator resistance	11.6 Ω
Rotor resistance	10.4 Ω
Stator inductance	0.579 H
Rotor inductance	0.579 H
Magnetizing inductance	0.577 H
Moment of inertia	0.002 Kg.m ²
Fraction coefficient	0.001 N.m.sec/rad

REFERENCES

- [1] Kranti Bhokare, Nishant Yewale and Shital Jamunkar "A review on direct torque control of induction motor," International Journal Of Core Engineering & Management (IJCEM), vol. 2, issue3, pp. 243-253, June 2016.
- [2] Vikramarajan Jambulingam "Direct torque control design for three phase induction motor," International Journal Of Engineering Devlopment and Research (IJEDR), vol. 4, issue1, pp. 281-290, 2016.
- [3] Lotfi El M'Barki, Moez Ayadi and Rafik Neji "Reduced torque ripple of IM by approach DTC," Intelligent Control and Automation, vol. 2, issue3, pp. 320-329, July 2011.
- [4] Y. C. Zhang, J. G. Zhu, Z. M. Zhao, W. Xu and D. G. Dorrell, "An improved direct torque control for three- level inverter-fed induction motor sensorless drive," IEEE Transactions on Power Electronics, Vol. 21, No. 5, pp. 1-12, 2010.
- [5] Z. Zhang, R. Tang, B. Bai, D. Xie, "Novel direct torque control based on space vector modulation with adaptive stator flux observer for induction motors", IEEE Transactions on Magnetics, Vol. 46, pp. 3133-3136, 2010.
- [6] Ranjit Kumar Bindala and Inderpreet Kaur "Performance of three phase induction motor of direct torque control using fuzzy logic controller," International Journal of Pure and Applied Mathematics, vol. 118, pp. 159-175, January 2018.



Dr. Hamdy Mohamed Soliman was born in Cairo, Egypt on 26th December 1970. He received B. Sc. in Electrical Power and Machine Engineering from Helwan Engineering, Helwan University in 1993. Master is from Shubra Engineering, Benha University. PhD Degree is from Cairo Engineering, Cairo University, Giza, Egypt in 2016.

He is a director genral of research and development of the Egyptian company for subway from 2016 - 2018.

Now he is working a lecture (teacher) in EL-Marg high institute for engineering and modern technology. His current research interests include electrical machines, power electronics, motor control and drive systems.